

# A SYMMETRICAL Z-AXIS GYROSCOPE WITH A HIGH ASPECT RATIO USING SIMPLE AND NEW PROCESS

S.S. Baek, Y.S. Oh, B.J. Ha, S. D. An, B. H. An, H. Song, C.M. Song  
Micro Systems Lab. Samsung Advanced Institute of Technology  
PO Box 111, Suwon, Korea  
Tel: 82-331-280-8266, e-mail: hsbak@saitgwsait.samsung.co.kr

## ABSTRACT

This paper reports on a symmetrical z-axis gyroscope, whose stiffness of sensing and driving mode is identical in spite of the fabrication and design errors. There is no need of the electrical tuning of frequencies for a high sensitivity because the effective masses of the driving and sensing directions are hardly changed. Furthermore, it is very simple to fabricate the gyroscope with a total chip size of  $3 \times 3.5 \times 1 \text{ mm}^2$  using only one mask. The gyroscope structure is fabricated on an anodic bonded  $40 \mu\text{m}$ -thick silicon on glass. After the top silicon is etched using a deep RIE, a part of the glass under the silicon structure is etched by HF for releasing the top silicon structure. Since the depth of the etched glass under the silicon structure is about  $20 \sim 30 \mu\text{m}$ , the damping and the stiction between the structure and the glass substrate are minimized. The minimum gap and the aspect ratio of this structure is  $2 \mu\text{m}$  and 20, respectively. Without an additional frequency tuning method, it is demonstrated that the difference between the two frequencies is about 85Hz, and the noise equivalent rate is  $0.01 \text{ deg/sec}$  at 50mTorr pressure.

## INTRODUCTION

The emergence of the new automotive and consumer applications such as a sensor for compensating the hand quiver in a video camera, a 3-D pointing device and a yaw rate sensor for a vehicle dynamics control etc., constantly increases the need for a small, inexpensive and high sensitive angular rate sensors.

Recently, several works on the micromechanical silicon gyroscope have been reported, and these gyroscopes are classified as two types depending on their operation principles. The first type is where the inertial mass is laterally driven and the Coriolis acceleration is vertically sensed (x-axis gyroscope)[1-4]. The second type is where the inertial mass is laterally driven and the Coriolis acceleration is laterally sensed (z-axis gyroscope)[5-8]. Generally, it is difficult to fabricate the two-fold axis gyroscope using a z-axis gyroscope and also it suffers from quadrature error[5]. However, there have recently been considerable works on the z-axis gyroscope as the fabrication is a simpler process than the x-axis gyroscope as well as being not sensitive to the fabrication error. Most of these gyroscopes should have a high mechanical quality factor and an additional tuning

method for a high sensitivity.

When the gyroscope is vibrating in its driving resonant frequency, its sensitivity is described as equation(1),

$$\Delta y = 2\Omega \frac{F_e Q_x}{m \omega_x} \frac{1}{\sqrt{(\omega_x^2 - \omega_y^2)^2 + \left(\frac{\omega_x \omega_y}{Q_y}\right)^2}} \quad (1)$$

where  $\Delta y$  is the displacement due to the Coriolis acceleration,  $\Omega$  the applied angular rate,  $F_e$  the driving force,  $m$  the inertial mass,  $Q_x$ ,  $Q_y$ ,  $\omega_x$  and  $\omega_y$  the mechanical quality factor and the resonant frequency in the driving and the sensing mode, respectively.

In order to improve the sensitivity of a vibratory gyroscope, it is necessary to match the resonant frequencies of the driving and the sensing modes ( $\omega_x \cong \omega_y$ ), and operate in a vacuum pressure for a high mechanical quality factor ( $Q_x$ ,  $Q_y$ ). The matching of the resonant frequency can be performed by controlling the electrical stiffness to lower the higher resonant frequency of the mismatched modes[9]. However, this electrical stiffness control causes the gyroscope to vibrate unstably, and it is not suitable for a mass production

This paper presents a z-axis gyroscope that employs the symmetrical spring to match the two frequencies without additional tuning method. Furthermore, the gyroscope needs a structure of high aspect ratio to obtain a high sensitivity and robustness, and therefore, is fabricated using the deep RIE with only one mask.

## WORKING PRINCIPLE AND STRUCTURE

### Working Principle

The structure of the designed gyroscope is shown in Figure 1. The dimensions of this structure is 3mm wide, 3.5mm long and  $40 \mu\text{m}$ -thick. Four symmetrical springs whose ends are attached at the external pad on glass suspends the moving structure. The gap between the moving structure and the fixed electrode is designed to be  $2 \mu\text{m}$  with  $500 \mu\text{m}$  length

The moving structure of the gyroscope consists of two

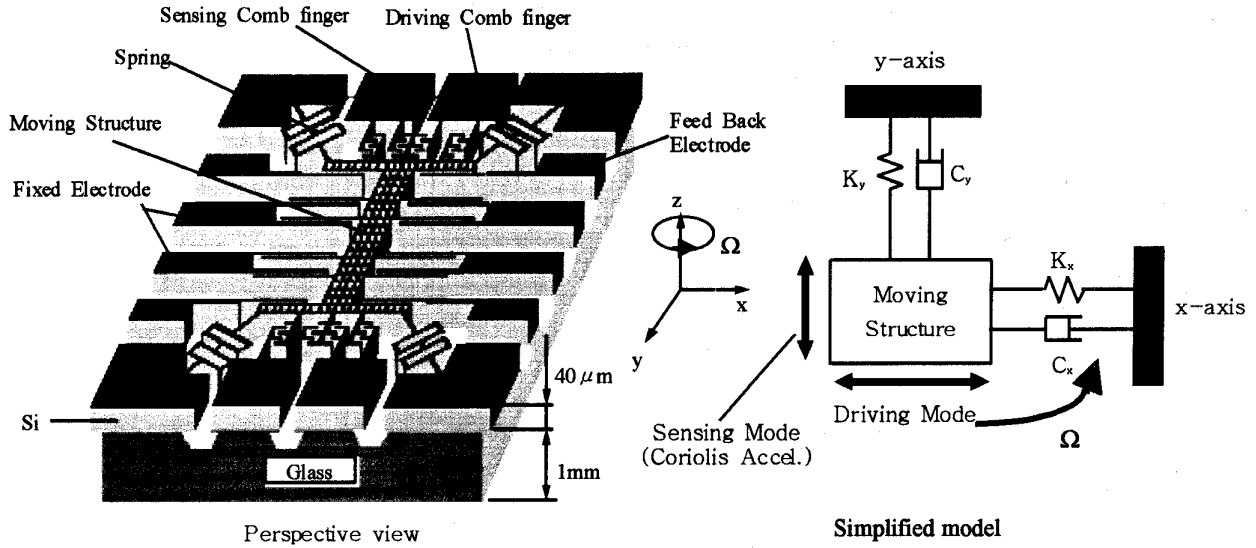


Fig.1 Illustration of symmetrical gyroscope

resonant modes; the driving mode(x axis) and the sensing mode(y axis). The moving structure is driven in the x direction by an electrostatic force which is generated by a driving voltage across the driving comb finger. The driving displacement( $\Delta x$ ) is sensed by capacitance change in the sensing comb finger, and is fed back to the driving comb finger so that the moving plate can be vibrated in its driving resonant frequency. The Coriolis acceleration arising from an angular rate around the z axis causes the moving structure to vibrate in a detection direction. The displacement( $\Delta y$ ) by the Coriolis acceleration can be differentially detected by the capacitance change between the moving structure and the fixed electrode.

### Symmetrical Spring

The symmetrical spring as shown in Fig.2, is introduced to coincide with the two frequencies (sensing and detection mode). Since the springs are symmetrical with respect to the driving direction(x axis) and the sensing direction(y axis), stiffness of both direction are equal to each other.

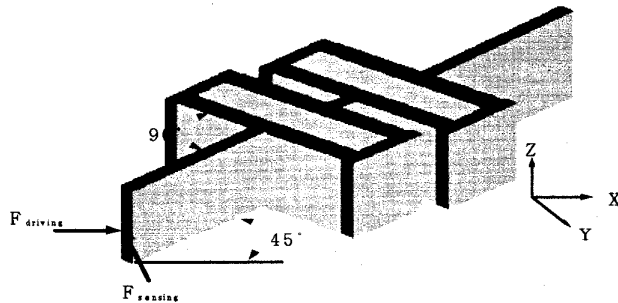


Fig.2 Symmetrical spring

Even though the thickness, width and length of the spring are changed by the fabrication error, two stiffness is changed equally.

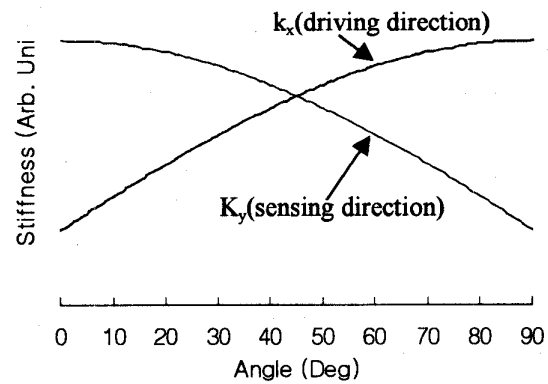


Fig.3 Stiffness vs. angle

Figure 3 shows the stiffness as a function of the angle between the x axis and the spring. The stiffness in the y axis is expressed as a normalized value calculated by the Castigliano's theorem[10]. As shown in this figure, stiffness in the driving mode coincides with the stiffness in the sensing mode at 45°. However, as angle increases, the stiffness in the driving mode is higher than the frequency in the sensing mode.

Generally, resonant frequency is represented in equation (2),

$$f = \frac{1}{2\pi} \sqrt{\frac{k}{m_{\text{effective}}}} \quad (2)$$

where  $k$  is the stiffness and  $m_{\text{effective}}$  the effective mass of the moving structure. If the stiffness of both is same, the difference of the resonant frequency will be affected by only the effective mass. This effective mass is hardly changed by a fabrication error. For example, if all dimensions are deviated by  $1\mu\text{m}$  from their designed values, the effective mass and the resonant frequency are changed by only 0.6% and 0.3% respectively from their designed values. Therefore, even though the absolute values of the resonant frequencies are changed considerably by a fabrication error, the difference of the two resonant frequencies can hardly be changed.

### FEM Modal Analysis

Figure 4 shows the FEM modal analysis for driving and sensing modes, respectively. The sensing mode was designed to have a little higher frequency than the driving mode because the frequency of the sensing mode can be lowered by a driving voltage. Generally, the frequency reduction by applying the DC voltage is represented in equation (3)[11],

$$f_y = \frac{1}{2\pi} \sqrt{\frac{1}{m} \left( k - \frac{\epsilon A V^2}{h^3} \right)} \quad (3)$$

where  $m$  is the mass of the moving structure,  $k$  the stiffness for the driving mode,  $\epsilon$  the dielectric constant,  $A$  the effective driving area,  $V$  the driving voltage and  $h$  the gap between the moving structure and the fixed electrode, respectively.

When a DC driving voltage of 2V is applied, the frequency of the sensing mode decreases from 5850Hz to 5770Hz. For this reason, the frequency of the sensing mode is designed to be 50Hz higher than the driving mode. This mismatch of the two frequencies is controlled by adjusting the length and the width of the structure or changing the angle between the spring and the  $x$  axis. For this gyroscope, the frequency mismatch is obtained by adjusting the angle to  $44^\circ$

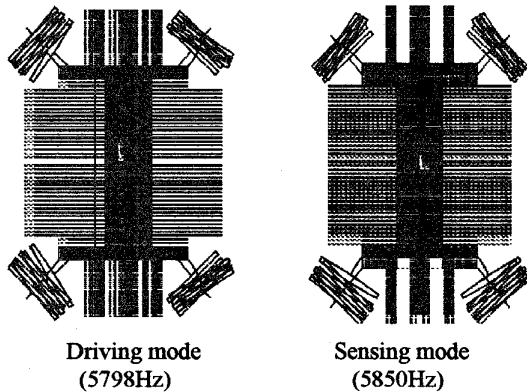


Fig.4 FEM modal analysis

### FABRICATION

The gyroscope was fabricated using a new bulk micromachining technology as shown in figure 5. A p-type silicon wafer (resistivity:  $0.001\sim 0.004\Omega\cdot\text{cm}$ ) is used for the top silicon wafer and the glass for the bottom substrate. The parasitic capacitance between the moving structure and the bottom substrate can be minimized by a nonconductive glass substrate. An additional doping process is not required to make the conductive structure because of a low resistive silicon wafer.

#### 1. Anodic bonding silicon and glass



#### 2. Lapping and polishing of silicon



#### 3. Deep RIE



#### 4. Glass etching and dicing



#### 5. Metal sputtering



#### 6. Wire bonding to ceramic package



Fig. 5 Fabrication flow

The process begins with an anodic bonding of silicon and glass at  $320^\circ\text{C}$ . The bonded silicon wafer is lapped and polished up to  $40\mu\text{m}$ . The next steps involved patterning and deep trench etching by ICP RIE(STS Inc.). The aspect ratio of the structure is 20. The top view is shown in Fig. 6. Etched wafer is diced and then a part of the glass below the moving structure is etched by HF for 4min.

Figure 7 shows the cross section of the gyroscope where the glass under the moving structure is etched. Since the gap between the moving structure and the bottom glass is about  $30\mu\text{m}$ , the damping and the stiction between the moving structure and the bottom glass can be minimized.

The next process is to deposit metal(Cr/Au) on each chip by sputtering. During the sputtering process, the metal covers on the whole surface of the top silicon and the bottom trench. However, due to the directional characteristics of the sputtering, a metal was not deposited on the glass under the moving structure. Therefore, each pad is completely isolated electrically. After the metal was deposited on the surface of the silicon, each sensor chip is packaged in a ceramic package and electrically connected by wire bonding. This process uses only one mask.

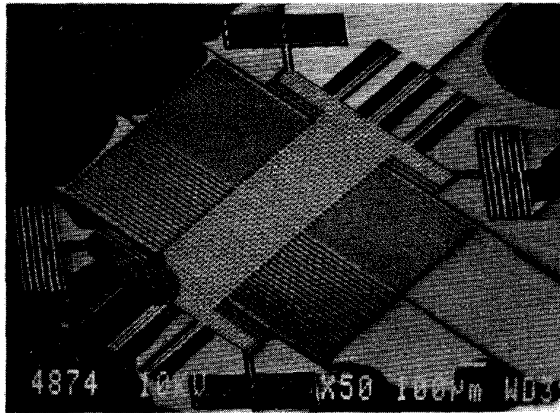
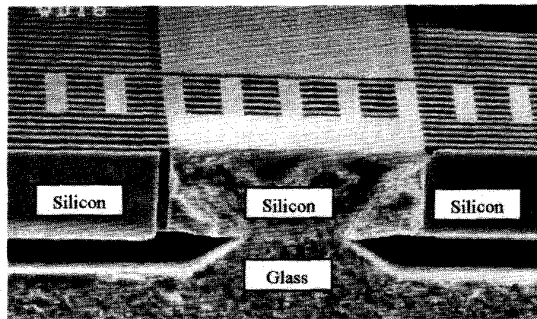


Fig.6 Top view of gyroscope



voltage of DC 2V with AC 1V is applied to the driving comb finger with a periodic chirp. The resonant frequencies can be detected by the capacitance change between the moving structure and the fixed electrode.

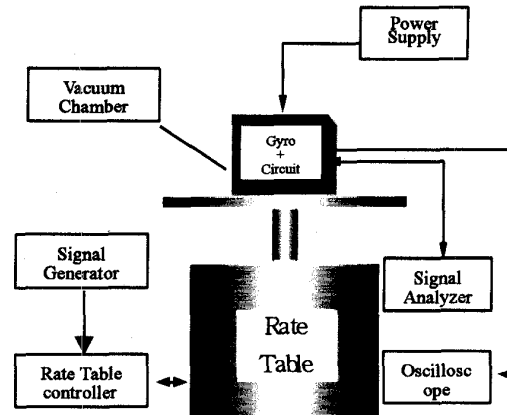


Fig. 8 Experimental setup

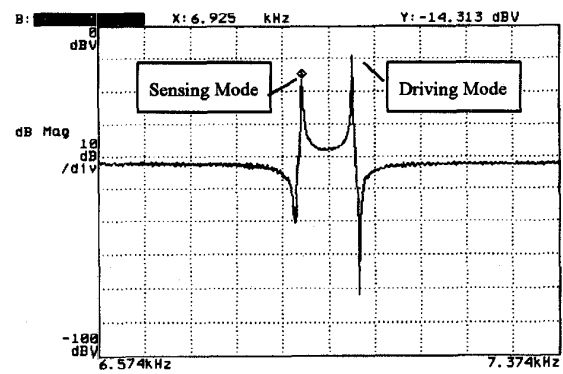


Fig. 9 Vibration characteristics

Figure 9 shows the vibration characteristics of

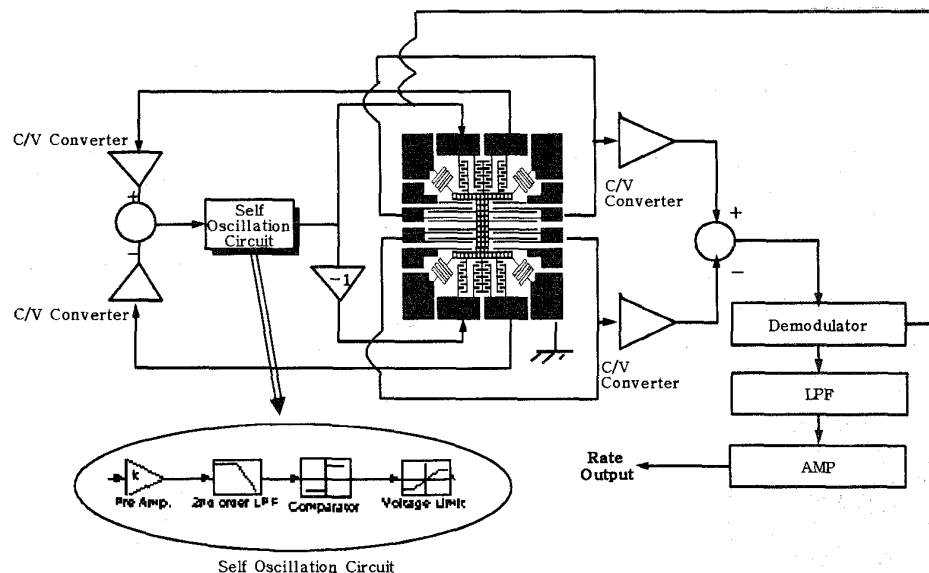


Fig. 10 Sensing scheme

The differential type of the comb finger detects the position of the mass along the oscillation direction. The position signal is amplified and filtered. Compared with the reference voltage, the signal is limited and then fed back to the driving comb finger. This feed-back loop is designed such that the mass is self-oscillated in a condition of driving resonant frequency. Therefore, a mass is always oscillated at the resonant frequency even though the resonant frequency is somewhat varied by the environment.

When the structure resonates, the displacement of the moving structure by the Coriolis acceleration produces the change of the capacitance between the moving structure and the fixed electrode. The change of electric charge in the capacitor is converted into the voltage by a C/V converter. To convert the charge of the capacitor to the voltage, the JFET is used. After removing the DC component through a high pass filter, the  $180^\circ$  out-of-phase signals are summed by the differential amplifier. The angular rate is recovered by demodulation and amplification by a phase-sensitive detection.

#### Performance of Gyroscope

The gyroscope uses resonant frequencies of 7010Hz in the driving mode and 6925Hz in the sensing mode without tuning. The driving voltages of DC 2V with AC 1V are applied to the driving comb fingers by means of a self-sustained oscillation loop. Figure 11 shows the output characteristics of a gyroscope in response to 5Hz, 1deg/sec. As seen in the figure, it is clear that the noise equivalent rate is about 0.01(deg/sec).

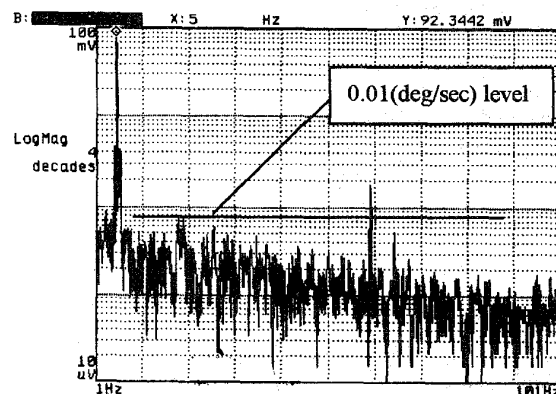


Fig. 11 Output characteristics of a gyroscope in response to 5Hz, 1deg/sec

#### CONCLUSION

A symmetrical micro gyroscope is designed, fabricated and tested. The new gyroscope introduces a symmetrical spring to match two resonant frequencies. Moreover, this structure is fabricated by a new and simple process with only one mask. The experimental results show that the difference between the two resonant frequencies is about 85Hz, and noise equivalent rate is about 0.01deg/sec without additional tuning method.

#### ACKNOWLEDGEMENTS

The authors would like to thank Kevin Lee of JIN SAN Scientific Co., Korea branch of STS Inc., for his arrangement in silicon deep RIE.

## REFERENCE

1. J. Berstein, M. Weinberg, 'A micro-machined comb-drive tuning fork gyroscope', *Proc. IEEE MEMS workshop '93*, pp. 143-148, Lauderdale, FL
2. Y. Oh, B. Lee, et al, 'A tunable vibratory microgyroscope', *Sensors and actuators, A64*, pp 51~57, 1998
3. S. An, Y. Oh, et al, 'Dual-axis microgyroscope with closed-loop detection' *Proc. IEEE MEMS workshop '98*, pp. 328-327, Hedelberg, Germany
4. W. Geiger, B. Folkmer, et al, 'A new silicon rate gyroscope', *Proc. IEEE MEMS workshop '98*, pp. 328-327, Hedelberg, Germany
5. A. Clark, R. T. Howe, 'Surface micromachined z-axis vibratory rate gyroscope', *Digest, Solid State Sensor & Actuator Workshop '96*, pp. 283-287, Hilton Head, SC
6. K. Y. Park, Y. Oh, et al, 'Laterally oscillated and force-balanced micro vibratory rate gyroscope supported by fish hook shape springs', *Proc. IEEE MEMS workshop '98*, pp. 272-277, Hedelberg, Germany
7. M. Lutz, W. Golderer, et al, 'A precision yaw rate sensor in silicon micromachining', *Proc. Transducers '97*, pp. 847-850, Chicago, Illinois
8. M. W. Putty, R. C. Gutierrez, et al., 'A Micromachined ring gyroscope', *Proc. Solid-state sensor and actuator workshop '94*, pp. 213-220, Hilton Head
9. B. Lee, Y. Oh, et al, 'A dynamically tuned vibratory micromechanical gyroscope-accelerometer', *Proc. of SPIE smart electronics and MEMS Vol.3242*, pp.86-95, 1997
10. G. K. Fedder, 'Simulation of microelectromechanical systems', Ph.D. Dissertation, U. C. Berkeley, USA, 1994
11. G. C. Turner, M. K. Andrews, 'Frequency stabilization of electrostatic oscillators', *Transducer '95*, pp. 624-626, Stockholm, Sweden